



Aalborg Universitet

AALBORG UNIVERSITY
DENMARK

Cooperative Control with Virtual Selective Harmonic Capacitance for Harmonic Voltage Compensation in Islanded MicroGrids

Micallef, A.; Apap, M. ; Spitero-Stanies, C.; Zapata, Josep Maria Guerrero

Published in:
Proceedings of the 38th Annual Conference of the IEEE Industrial Electronics Society

DOI (link to publication from Publisher):
[10.1109/IECON.2012.6389037](https://doi.org/10.1109/IECON.2012.6389037)

Publication date:
2012

Document Version
Early version, also known as pre-print

[Link to publication from Aalborg University](#)

Citation for published version (APA):
Micallef, A., Apap, M., Spitero-Stanies, C., & Guerrero, J. M. (2012). Cooperative Control with Virtual Selective Harmonic Capacitance for Harmonic Voltage Compensation in Islanded MicroGrids. In Proceedings of the 38th Annual Conference of the IEEE Industrial Electronics Society (pp. 5619 - 5624). IEEE Press. I E E E Industrial Electronics Society. Annual Conference. Proceedings <https://doi.org/10.1109/IECON.2012.6389037>

General rights

Copyright and moral rights for the publications made accessible in the public portal are retained by the authors and/or other copyright owners and it is a condition of accessing publications that users recognise and abide by the legal requirements associated with these rights.

- ? Users may download and print one copy of any publication from the public portal for the purpose of private study or research.
- ? You may not further distribute the material or use it for any profit-making activity or commercial gain
- ? You may freely distribute the URL identifying the publication in the public portal ?

Take down policy

If you believe that this document breaches copyright please contact us at vbn@aub.aau.dk providing details, and we will remove access to the work immediately and investigate your claim.

Harmonic Voltage Compensation in Islanded MicroGrids

A. Micallef, M. Apap and C. Spiteri-Staines

Department of Industrial Electrical Power Conversion
University of Malta
Msida, MSD 2080, Malta
alexander.micallef@um.edu.mt

J. M. Guerrero^{+,*}

⁺ Institute of Energy Technology
Aalborg University, Denmark
^{*} Department of Automatic Control Systems Universitat
Politecnica de Catalunya, Barcelona 08036, Spain
joz@et.aau.dk

Abstract — This paper focuses on the islanded operation of microgrids. In this mode of operation, the microsources are required to cooperate autonomously to regulate the local grid voltage and frequency. Droop control is typically used to achieve this autonomous voltage and frequency regulation. Inverters having LCL output filters would cause voltage distortion to be present at the PCC when non-linear current is supplied to the load due to the voltage drop across the grid side inductor. Techniques to reduce the output voltage distortion typically consist of installing either passive or active filters to selectively compensate harmonic frequencies. However, by adding suitable control strategies to the inverters connected to the microgrid, the power quality of the microgrid can be improved without the installation of any additional equipment. In this paper, a capacitive virtual impedance loop, implemented in each of the microsource inverters, is proposed so as to dampen the voltage harmonics at the PCC. Simulation results are presented showing the suitability of the proposed algorithm in dampening the PCC voltage harmonics.

Keywords - microgrids, harmonic compensation, harmonic current sharing, islanded operation, capacitive virtual impedance

I. INTRODUCTION

The recent shift in paradigm towards the decentralization of electricity generation has effectively increased the penetration of distributed generation (DG). Microgrids are becoming an important concept to integrate DG and distributed energy storage systems [1]. When paralleling multiple inverters, that are capable of operating in both grid connected and islanding mode, a droop control scheme [1 - 4] is typically used in which the voltage and frequency of each inverter are adjusted in order to control active and reactive power. Droop control employs locally measured variables namely to achieve equal p.u. real and reactive power sharing when operating in islanded mode. Control algorithms for inverters having LCL output filters typically control the inverter side inductor current and the capacitor voltage. The voltage drop on the grid side inductors causes attenuation and phase difference at the PCC when supplying linear loads. Any non-linear current supplied to the load would cause voltage distortion to be present at the PCC due to the voltage drop across the grid side inductor.

Harmonic currents drawn by non-linear loads may cause stability issues due to any resonances present on the microgrid [5]. In islanded mode, the inverters participating in regulating the voltage and frequency of the microgrid form a weak grid.

Harmonic current flow thus causes voltage distortion to appear at the PCC. Harmonic damping techniques must be considered to reduce the harmonic distortions. Several voltage harmonic reduction techniques can be extended from the grid connected systems. These typically consist of installing either passive or active filters to selectively compensate harmonic frequencies. However, by adding proper control strategies to the inverters connected to the microgrid, these can be used to improve the power quality of the microgrid [5].

The authors in [6] propose a compensation scheme in which a sinusoidal voltage is produced at the PCC by operating the inverter using a non-sinusoidal PWM control. This results in the cancellation of the nonlinear drop across the line impedance to achieve a sinusoidal voltage at the PCC. Although the concept to generate a signal in opposition to the harmonic drop is simple and effective in reducing the voltage harmonics, the results shown are for only for a single inverter connected to the microgrid. Since the proposed algorithm is directly based on regulating the voltage harmonics at the PCC, the introduction of multiple inverters each with this capability could pose a serious problem towards the stability of the complete system. Also the control loops do not include the capability to regulate the current output from the inverter. No further solutions are available in literature for the reduction of harmonics in islanded mode for single phase devices.

A secondary waveform control approach is proposed in [7] to reduce the harmonics in a three phase system with LC filters. This approach redistributes the harmonics over a wider frequency range to reduce the harmonic voltage amplitudes and hence improve the voltage THD. The communications bandwidth is minimized with the help of Park transformation. Such an implementation can also be adapted to single phase systems however minimization of the communications bandwidth in such cases could be a complex task. A harmonic conductance-harmonic VAR droop was proposed by the authors of [5], [8] and [9] with the main difference being the implementation. The G-Q droop damps the harmonic resonances and distributes the harmonic filtering among the microsources. The authors of [5] use a droop for all the harmonic power supplied by the inverter while the authors in [8] and [9] apply selective harmonic compensation. However, the introduction of an additional droop control loop makes the design of the droop gains of the inverters even more complex

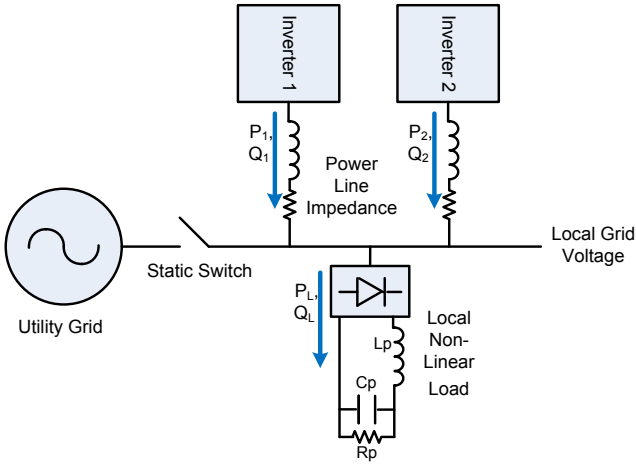


Fig. 1. Microgrid Hardware Setup

as this loop may affect the dynamics of the real and reactive power sharing loop.

In this paper, a capacitive virtual impedance loop is proposed so as to dampen the voltage harmonics at the PCC. The paper is organized as follows. In Section II, a description of the implemented system was given which includes the inverter control loops and the complete microgrid setup. Section III contains a description of the capacitive virtual impedance loop that was implemented. A summary of the simulation results was given in Section IV, showing the suitability of the capacitive virtual impedance loop proposed in this paper to dampen the voltage harmonics at the PCC.

II. ISLANDED OPERATION OF PARALLEL INVERTERS FORMING A MICROGRID

The islaned microgrid consists of two parallel inverters, each with LC output filters and isolation transformers to provide the grid side inductance thereby effectively forming an isolated LCL output filter. A local non-linear load, consisting of a single phase rectifier with smoothing capacitor, was connected to the microgrid as shown in the system block diagram in Fig. 1. When the utility grid is present, the static switch (SS) connects the microgrid to the utility grid and handles the synchronization process together with the microgrid central controller (MGCC). For operation in islanding mode, the SS is open and the inverters operate autonomously to regulate the local grid voltage and frequency. A contactor at the output of each inverter allows for synchronization of the inverter via a PLL to the voltage at the PCC, before any power transfer to the microgrid can be performed so as to minimize the impact that the inverter has on the rest of the microgrid. The power lines connecting the inverters to the local grid were represented via the short transmission line model.

A. Outer Droop Control Loop

Each microsource inverter is capable of operating in either grid connected or islaned mode depending on the state of the static switch and the presence of the utility grid. For simplicity

in this simulation, the state of operation of the microsources is

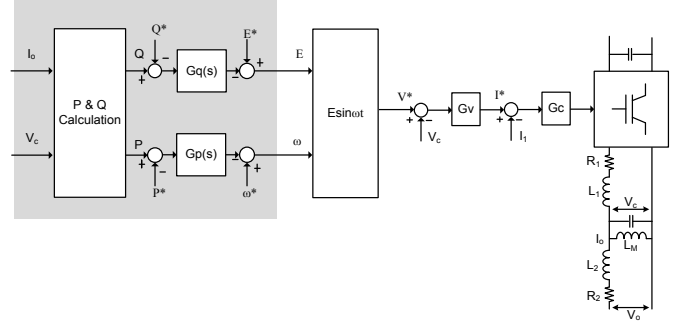


Fig. 2. Microsource Inverter control block diagram for islaned mode.

determined by the central controller which also determines the state of the SS. Fig. 2 illustrates the block diagram of the control loop implemented in these inverters that enables the operation in islaned mode. In islaned mode, real power is supplied by varying the real power against frequency ($P-\omega$) while in grid connected mode the real power is supplied by varying the real power against the phase ($P-\Phi$), as the frequency is fixed by the grid. The controller evaluates the actual real and reactive power output of the inverter in either mode and sends these values to the droop control algorithm from which the reference voltage waveform is generated. The droop control functions in islanding mode can be mathematically expressed as:

$$\omega = \omega^* - (k_{dP}S + k_{pP})(P - P^*) \quad (1)$$

$$E = E^* - (k_{dQ}S + k_{pQ})(Q - Q^*) \quad (2)$$

where P is the actual real power output of the microsource; Q is the actual reactive power output of the microsource; k_{pP} and k_{pQ} are the droop gains; and k_{dP} and k_{dQ} are the derivative gain terms. Proportional derivative control is used as the principle behind droop control is to allow an error in the voltage and frequency set-points. This implies that integral terms would cause the system to become unstable. In islanding mode P^* and Q^* are typically set to zero as the load determines the amount of real and reactive power that the inverters will supply.

B. Inner Control Loop Design

The voltage control loop regulating the inverter output voltage is common for both operation modes. The proposed inner controllers, based on the stationary reference frame, consist of a voltage and an inner current loop. The voltage and

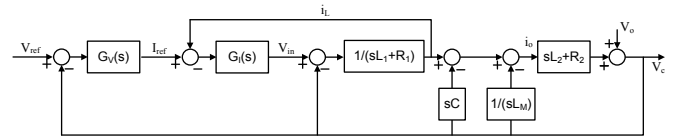


Fig. 3. Block diagram of the inner loops. The plant consists of an LC filter and an isolation transformer to interface with the microgrid. L_M , L_2 and R_2 are the transformer parameters namely the magnetization inductance, leakage inductance and winding resistance. $G_V(s)$ and $G_I(s)$ are the voltage and current controller transfer functions respectively.

current control loops are both based on the Proportional-Resonant (PR) controller [11 - 13]. The PR controller was preferred over the various voltage PID controllers available in literature [10] as the latter have various disadvantages when the control variable is sinusoidal and the controlled variable is not transformed to the synchronous frame. In addition, simulations carried out with the system in Fig. 1 comparing the performance of the PR to a two-degrees of freedom PID have shown superior performance of the PR by achieving a lower voltage THD at the output of the LC filter.

In order to analyze the closed loop dynamics and determine the controller gains required, a linear model of the system was obtained as shown in Fig. 3. V_{ref} is the voltage reference that is obtained from the outer droop control loop, i_L is the current through inductor L_1 , L_1 is the value of the output inductor, R_1 is the parasitic resistance of the output inductor, C is the value of the filter capacitor. Initially the parameters for the current controller $G_i(s)$ are obtained by considering the inner loop shown in Fig. 3 and by using root locus techniques while assuming V_c as constant. The voltage controller parameters can then be obtained by simplifying the block diagram of Fig. 3 and through the use of root locus techniques. The bode plot of the simulated closed loop system is shown in Fig. 4. In addition to the fundamental resonant control transfer function, resonant terms for each harmonic that will be compensated were introduced in the voltage and current transfer functions. These are added so as to provide closed loop control of the selected harmonics. The gains for the harmonic elements were also obtained via the described root locus design procedure. The transfer functions of the voltage and current controllers can be given by [11]:

$$G_v(s) = K_{pv} + \frac{k_{iv}s}{s^2 + 2\omega_{cv}s + \omega^2} + \sum_{h=3,5,7,9,11} \frac{k_{ivh}s}{s^2 + 2\omega_{cvh}s + \omega_h^2} \quad (3)$$

$$G_i(s) = K_{pi} + \frac{k_{is}}{s^2 + 2\omega_{cl}s + \omega^2} + \sum_{h=3,5,7,9,11} \frac{k_{ilh}s}{s^2 + 2\omega_{clh}s + \omega_h^2} \quad (4)$$

where K_{pv} and K_{pi} are the proportional gain terms, k_{iv} and k_{il} are the fundamental resonant gain terms, ω_{cv} and ω_{cl} are the fundamental resonant bandwidth control terms, ω is the fundamental resonant frequency, k_{ivh} and k_{ilh} are the harmonic resonant gain terms, ω_{cvh} and ω_{clh} are the harmonic resonant bandwidth control terms and ω_h is the resonant frequency at the harmonic.

III. CAPACITIVE VIRTUAL IMPEDANCE LOOP

Inverters having an output LCL filter cause voltage distortions at the PCC when supplying non-linear loads due to

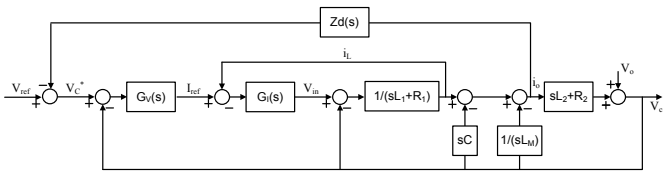


Fig. 4. Block diagram of the inner loops with virtual impedance $Z_d(s)$.

the voltage drops on the grid side output inductor and the power line impedances. Instead of introducing additional passive or active filters to selectively attenuate the harmonics at the PCC, a capacitive virtual impedance loop is proposed in this paper to dampen these voltage harmonics. The basic principle of the capacitive virtual impedance loop is to compensate for the non-linear inductive voltage drop by introducing a capacitive component and effectively distorting the output voltage of the inverter $V_c(s)$. The concept of virtual impedance loops is available in literature and was proposed to achieve equal power sharing [1], [2], [10] through the use of inductive impedance loops for systems having an LC output filter. To the authors' knowledge, there are no references of such a harmonic compensation solution available in literature.

The block diagram of Fig. 4 shows how the capacitive virtual impedance loop interacts with the inner control loops of the inverter. From this figure, the voltage across the filter capacitor can now be expressed as:

$$V_c^*(s) = V_{ref}(s) - i_o(s)Z_d(s) \quad (5)$$

where $V_c^*(s)$ is the desired output of the inverter, $V_{ref}(s)$ is the fundamental reference from the droop control loop, $i_o(s)$ is the output current supplied to the load by the inverter and $Z_d(s)$ is virtual impedance transfer function. Hence, the voltage reference of the inner loops now takes into consideration the virtual voltage drop across the virtual impedance.

The virtual impedance transfer function $Z_d(s)$ consists of a series of band-pass filters tuned at each harmonic frequency to be dampened (3rd, 5th, 7th, 9th and 11th) and cascaded with a capacitive impedance block. Thus, $Z_d(s)$ can be expressed by:

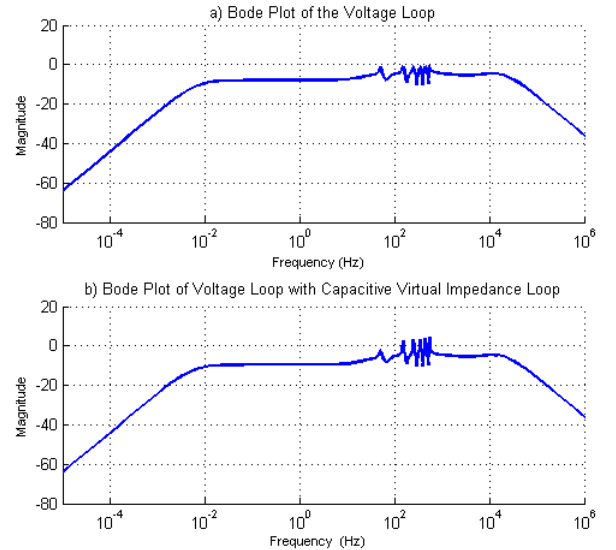


Fig. 5. a) Bode plot of the closed loop transfer function $\frac{V_c(s)}{V_{ref}(s)}$ without the virtual impedance loop for the PR controller parameters given in Table II. b) Bode plot of the closed loop transfer function $\frac{V_c(s)}{V_{ref}(s)}$ with the virtual impedance loop for the PR controller parameters given in Table II.

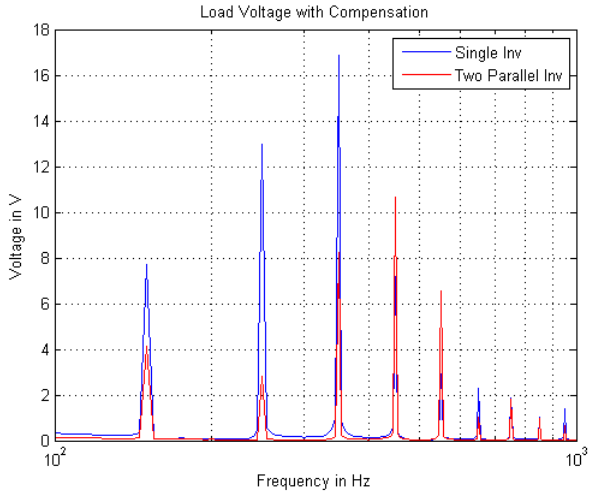


Fig. 6. Voltage Harmonics at the PCC without the Capacitive Virtual Impedance Loop.

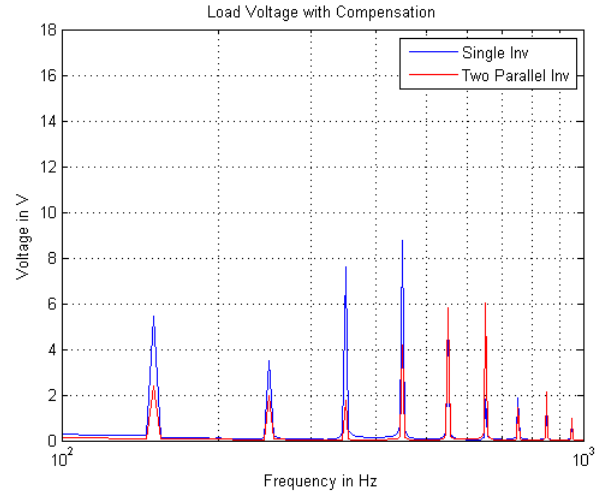


Fig. 8. Voltage Harmonics at the PCC with the Capacitive Virtual Impedance Loop.

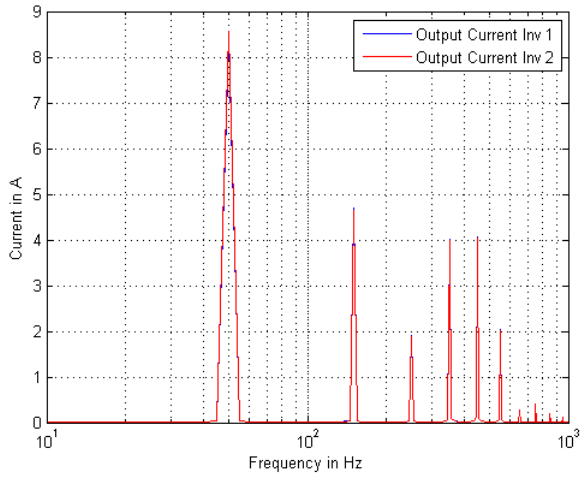


Fig. 7. Non-Linear current sharing by the inverters without the Capacitive Virtual Impedance Loop at steady state.

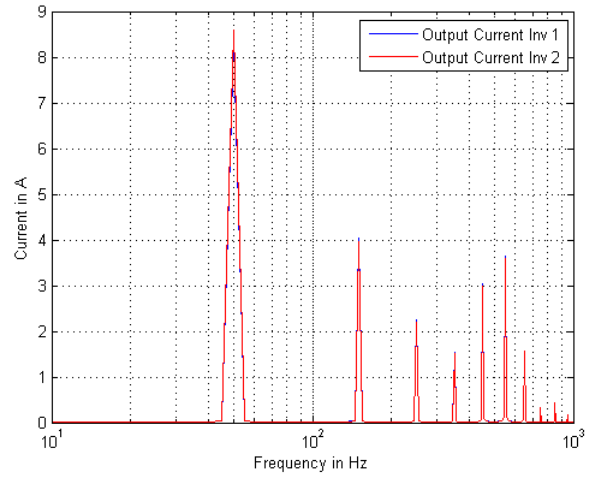


Fig. 9. Non-Linear current sharing by the inverters with the Capacitive Virtual Impedance Loop at steady state.

$$Z_d(s) = \sum_{h=3,5,7,9,11} \frac{k_{ih}s}{s^2 + 2\omega_{ch}s + \omega_h^2} \cdot \frac{k_{ch}}{s} \quad (6)$$

where k_{ih} is the harmonic resonant gain terms, ω_{ch} is the harmonic resonant bandwidth control term, ω_h is the resonant frequency at the harmonic and k_{ch} is the capacitive impedance at that harmonic.

The voltage control loop as shown in Fig. 3, without the virtual impedance loop, was designed to exhibit a closed loop response as shown in Fig. 5a. A 1Ω series resistor was considered in this implementation to reduce the selectivity of the output LCL filter. The gain over the bandwidth shown is always less than 4dB except at the resonant frequencies where the gain is 0dB. The introduction of the additional capacitive virtual impedance loop does not compromise the operation of the inner control loops. This can be observed from the bode plot of Fig. 5b which exhibits a similar closed loop response to that of Fig. 5a. However, in this case the gains at the resonant frequencies are now higher than 0dB. Hence the overall effect

of the virtual impedance loop is to provide harmonic voltages to the inner loops that compensate the drop due to the inductive grid side impedance.

IV. RESULTS

The aim of this section is to verify the effectiveness of the capacitive virtual impedance loop in dampening the voltage harmonics. The two inverters, were connected sequentially to the microgrid (at $t=0s$ and $1s$ respectively) while operating in islanded mode. The microsource inverters are required to supply a local single phase rectifier with smoothing capacitor ($L_p = 84\mu H$, $C_p = 235\mu F$ and $R_p = 25\Omega$). Inverter 1 is connected at $t=0$ and sets the microgrid voltage and frequency according to the droop control. It is assumed that each inverter can handle the load present on the microgrid. The other inverter synchronizes with the microgrid voltage and is connected after $1s$. Under these conditions, it is expected that the inverters share equally the active and reactive power demanded by the load. The simulation model parameters are given in Table I.

Fig. 6 shows the voltage harmonics at the PCC for simulations that were carried out without the capacitive virtual impedance loop. The non-linear current drawn from the LCL filter causes voltage drops across the grid side inductance, resulting in voltage distortion at the PCC. The voltage THD for a single inverter connected to the microgrid was of 7.8%, while the THD for two inverters was of 5.2%. The reduction in THD by the addition of another inverter shows that as the inverters share the non-linear current between them, the effect on the voltage at the PCC is reduced. The current sharing between the inverters at steady state is shown in Fig. 7. This figure shows that the current sharing even of the current harmonics occurs even without the addition of the virtual impedance loop.

Simulations were then carried out under the same conditions listed in Table I but with the additional virtual impedance loop in the inverter controllers. The voltage harmonics obtained at the PCC in this case were reduced as shown in Fig. 8. The voltage THD for a single inverter present on the microgrid was reduced to 4.7% while the THD for two inverters was reduced to 3.3%. The current sharing between the inverters at steady state is shown in Fig. 9. This figure shows that the introduction of the virtual impedance loop does not affect the current sharing between the inverters. From Fig. 7 and Fig. 9, the reduction in the voltage THD can be attributed to the redistribution of the current harmonics. Simulation parameters for the virtual impedance loop are given in Table II.

TABLE I. SIMULATION PARAMETERS

Inverter	Power Line Parameters		Inverter Parameters					
	R_{TX_n}	L_{TX_n}	R_1	L_1	C_1	R_2	L_2	L_M
	Ω	mH	Ω	mH	μF	Ω	mH	H
1	0.0175	0.005	0.184	0.92	18.4	0.184	0.92	0.92
2	0.0525	0.016	0.200	1.00	20.0	0.200	1.00	1.00

V. CONCLUSIONS

This paper considers the voltage harmonics at the PCC due to non-linear loads supplied by inverters operating in islanding mode. Tests carried out for a single phase rectifier with smoothing capacitor have shown that the THD reached 7.8% for the case of a single inverter connected on the microgrid. Instead of including additional passive or active filters to the microgrid, capacitive virtual impedance loops were proposed to dampen the voltage harmonics at the PCC. These use selective filtering of the harmonics from the grid side output current of the inverter to generate a voltage vector that opposes the voltage drop across the output filter grid side inductive impedance. Simulation results have shown that the proposed loop achieved a significant reduction in the THD at the PCC thereby indicating the effectiveness of the proposed algorithm to dampen the voltage harmonics.

TABLE II. PARAMETERS OF INNER VOLTAGE AND CURRENT CONTROLLERS AND CAPACITIVE VIRTUAL IMPEDANCE LOOP

Parameter	Value	Units
k_{pV}	10	
k_{pI}	10	
k_{iV}	615	
k_{iI}	2512	
k_{iVh}	$h \times 615$	
k_{iIh}	$h \times 2512$	
k_{c3}	342	
k_{c5}	1042	
k_{c7}	2120	
k_{c9}	3611	
k_{c11}	5734	
ω_{cVh}	$h \times 3.14$	rad/s
$\omega_{cIh}, \omega_{ch}$	$h \times 31.4$	rad/s
ω_h	$h \times 100\pi$	rad/s
ω_{cV}	3.14	rad/s
ω_{cI}	31.4	rad/s
ω	100π	rad/s

REFERENCES

- [1] J. M. Guerrero, J. C. Vasquez, J. Matas, L. G. de Vicuña, and M. Castilla, "Hierarchical Control of Droop-Controlled AC and DC Microgrids—A General Approach Toward Standardization", *IEEE Trans. Ind. Electron.*, vol. 58, no. 1, pp.158 -172, 2011.
- [2] J. M. Guerrero, L. Hang, and J. Uceda, "Control of Distributed Uninterruptible Power Supply Systems", *IEEE Trans. Ind. Electron.*, vol. 55, no. 8, pp. 2845 - 2859, 2008.
- [3] A. Tuladhar, H. Jin, T. Unger, and K. Mauch, "Control of parallel inverters in distributed AC power systems with consideration of line impedance effect," *IEEE Trans. Ind. Appl.*, vol. 36, no. 1, pp. 131–138, 2000.
- [4] J. A. P. Lopes, C. L. Moreira, and A. G. Madureira, "Defining control strategies for microgrids islanded operation," *IEEE Trans. Power Syst.*, vol. 21, no. 2, pp. 916–924, 2006.
- [5] T. L. Lee and P. T. Cheng, "Design of a new cooperative harmonic filtering strategy for distributed generation interface converters in an islanding network", *IEEE Trans. Power Electron.*, vol. 22, no. 5, pp.1919- 1927 , 2007.
- [6] H. Patel, and V. Agarwal, "Control of a stand-alone inverter-based distributed generation source for voltage regulation and harmonic compensation," *IEEE Trans. Pow. Del.*, vol. 23, no. 2, pp. 1113-1120, Apr. 2008.

- [7] W. Xiongfei, J.M. Guerrero, F. Blaabjerg, and C. Zhe, "Secondary voltage control for harmonics suppression in islanded microgrids", *IEEE Power and Energy Society General Meeting*, 2011.
- [8] M. Savaghebi, A. Jalilian, J.C. Vasquez and J.M. Guerrero, "Selective compensation of voltage harmonics in an islanded microgrid", *IEEE Power Electron., Drive Syst. and Tech. Conf. (PEDSTC)*, pp. 279 - 285, 2011.
- [9] M. Savaghebi, A. Jalilian, J.C. Vasquez, J.M. Guerrero and T.-L. Lee, "Voltage harmonic compensation of a microgrid operating in islanded and grid-connected modes", *Proc. IEEE Iranian Conf. Elec. Eng. (ICEE)*, 2011.
- [10] J. M. Guerrero, J. Matas, L. G. de Vicuña, M. Castilla, and J. Miret, "Output Impedance Design of Parallel-Connected UPS Inverters With Wireless Load-Sharing Control", *IEEE Trans. Ind. Electron.*, vol. 52, no. 4, pp. 1126 - 1135, 2005.
- [11] F. Blaabjerg, R. Teodorescu and M. Liserre, "Overview of control and grid synchronization for distributed power generation systems", *IEEE Trans. Ind. Electron.*, vol. 53, no. 5, pp.1398 -1409, 2006.
- [12] Y. Shuitao, L. Qin, F.Z. Peng, and Q. Zhaoming, "A Robust Control Scheme for Grid-Connected Voltage-Source Inverters", *IEEE Trans. Ind. Electron.*, vol. 58, no. 1, pp. 202 - 212, 2011.
- [13] M. Castilla, J. Miret, J. Matas, L. G. Vicua and J. M. Guerrero, "Control design guidelines for single-phase grid-connected photovoltaic inverters with damped resonant harmonic compensators", *IEEE Trans. Ind. Electron.*, vol. 56, no. 11, pp.4492 - 4501, 2009.